

Hydrothermal Ageing of Metallocene Polyethylene Films in Presence of Grafted Amine Stabilizers

Radu Setnescu · Mustapha Kaci · Nadjet Dehouche ·
Tanța Setnescu · Lounis Nasri · Traian Zaharescu

Received: 13 July 2013 / Accepted: 7 November 2013 / Published online: 16 November 2014
© King Fahd University of Petroleum and Minerals 2014

Abstract The hydrothermal degradation at 90 °C in distilled water of metallocene linear low density polyethylene films (mLLDPE) has been studied using low density polyethylene (LDPE) for comparison. FTIR spectroscopy, DSC and chemiluminescence techniques were used for investigation of the hydrothermal ageing-induced changes. The stabilization effect of a commercially available HALS, namely Sanduvor PR 31, able to graft on polyolefin structures has been also studied, as well. It was found that intense oxidation process occurs in the case of LDPE: hydroxyl, carbonyl and unsaturated groups were identified in FTIR spectra. mLLDPE reference films presented considerably higher stability as compared to LDPE ones, this behaviour being assigned to the structural peculiarities. Sanduvor PR 31 induced higher stability in LDPE, possibly by grafting mechanism, but it did not present a significant effect in the case of mLLDPE. Besides a possible antagonist interaction with the process stabilizer or a graft-hindering effect of the alkyl side groups, the intrinsic higher stability of the mLLDPE which offers less active sites for grafting could be supposed to explain this lower effectiveness.

Keywords Metallocene LLDPE · Hydrothermal ageing · FT-IR · DSC · Chemiluminescence

1 Introduction

During their service life, the polymer materials are subjected to degradation processes, which can be initiated by different stress factors, such as heat, light, weathering, radiation, mechanical efforts, chemical attack, microorganisms, a.s.o. [1]. As a result, the functional properties of the items incorporating plastics are steadily worsened, and finally, the failure is produced. For security and economic reasons, it is necessary to ensure adequate lifetime of products by addition of different stabilizers (antioxidants, photo-stabilizers, antirad agents, a.s.o) to extend the lifetime of widely used polymers such as polyethylene, polypropylene or their copolymers [2–9].

Hydrothermal degradation occurs when hot water and eventually air are in contact with the polymeric materials. Such type of stress is found in the case of hot water pipes and tubes, geomembranes, and in treatment of some wastes in subcritical or in supercritical conditions (supercritical water presents remarkable transport properties), in oxidative or non-oxidative conditions [10].

Hydrothermal ageing of polyethylene has been studied in relation to its application to hot water pipes. Medium density polyethylene (MDPE) and high density polyethylene (HDPE) were intensively studied in ageing experiments under hydrothermal and pressure conditions [11–14]. The fracture mechanisms of the XLPE in hot water pipes subjected to hydrothermal ageing were found to be closely related to the degradation state of the [13]. In high ageing stages, the antioxidant is totally depleted and the polymer becomes brittle due to chemical oxidation processes. It was

R. Setnescu · T. Setnescu
Faculty of Sciences and Arts, Department of Sciences,
Valahia University of Targoviste, Bd. Unirii 18-22, 130082
Târgoviste, Jud. Dâmbovită, Romania

R. Setnescu · T. Setnescu · T. Zaharescu
National R&D Institute for Electrical Engineering (ICPE-CA),
313 Splaiul Unirii, Sector 3, 030138 Bucharest, Romania

M. Kaci (✉) · N. Dehouche · L. Nasri
Laboratory of Advanced Polymeric Materials (LMPA),
Faculty of Technology, Abderrahmane Mira University,
Route de Targa-Ouzemmour, 06000 Bejaia, Algeria
e-mail: kacimu@yahoo.fr

also mentioned that the depletion of antioxidant in stabilized polyethylene occurs in a first stage by internal precipitation, then by migration in the environment [11]. The lifetime of the pipes and tubes for hot water has been evaluated using either antioxidant concentration profiles [15] or OIT-based models [11].

The hydrothermal studies focused on polyethylene degradation in geomembranes aimed to evaluate the lifetime through accelerated tests at elevated temperatures in immersion in distilled or tap water as well as in simulation or real leachates [16–21]. It was emphasized that the main degradation process is oxidation, while the antioxidant is depleted by different physical or chemical mechanisms [17, 18].

However, the data concerning the behaviour of metallocene polyethylene in hydrothermal ageing conditions are scarce.

The present study deals with the hydrothermal ageing of metallocene linear low density polyethylene (mLLDPE) films in comparison with low density polyethylene (LDPE), a topics which is of interest for various applications involving these materials, such as mulching films durability [22], ageing in hot water conditions [23, 24], geological applications [15], abiotic degradation and environmental persistence of the polymeric materials [25].

This work aims also to characterize the effect of a hindered amine stabilizer (HALS) compound that was found to graft on polymeric chains under UV light irradiation, hence providing improved stability and less migration phenomena during the service life of the polymeric materials [26–30].

2 Experimental

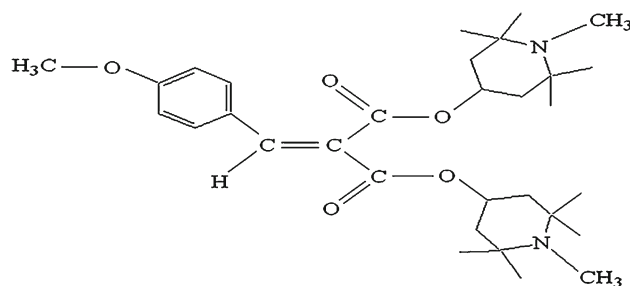
2.1 Materials

Low density polyethylene (LDPE) and metallocene linear low density polyethylene (mLLDPE) were used in the form of films of an average thickness of about 90 μm .

LDPE used is a homopolymer produced by radical polymerization by BP Chemicals (Belgium) and commercially available under the trade name Novex LD1407 KD. The main physical characteristics of the polymer are melting flow index (MFI) = 0.75 g/10 min, Vicat softening temperature = 94 $^{\circ}\text{C}$ and density = 0.924 g/cm^3 .

mLLDPE is an ethylene–hexene copolymer produced by Exxon Mobil (Saudi Arabia) using metallocene catalysts and commercially available under the trade name Exceed 1018. It has been kindly provided by Sofiplast, an enterprise of ENPC group located in Sétif (Algeria). This mLLDPE presents a MFI of 1 g/10 min, a melting point of 118 $^{\circ}\text{C}$ and a density of 0.918 g/cm^3 .

Films of $90 \pm 5 \mu\text{m}$ were prepared by blown extrusion process using a Battenfeld R160 SV type with L/D ratio



Scheme 1 The chemical structure of the stabilizer Sanduvor PR 31 (Clariant)

of 24. For LDPE, the temperature profile along the barrel ranged between 160 and 200 $^{\circ}\text{C}$, while in the die, the temperature decreased from 200 to 180 $^{\circ}\text{C}$. For mLLDPE, the temperature along the barrel was raised to 220 $^{\circ}\text{C}$. In both cases, the rotation speed was 35 rpm. The pulling speed of the film was 5 m/min, and the chilling was realized by air flow.

A HALS, namely Sanduvor PR 31, herein after referred as PR 31, manufactured by Clariant Company (France), in concentration of 0.3 wt% was added as stabilizer during the film fabrication. The chemical structure of this additive is shown in Scheme 1. Free of PR 31, both mLLDPE and conventional LDPE films were also prepared in similar experimental conditions, for comparative purposes.

2.2 Instruments and Methods

2.2.1 Hydrothermal Ageing

The hydrothermal ageing has been carried out by the immersion of LDPE and mLLDPE films in stainless steel thermostatic bath containing distilled water at 90 $^{\circ}\text{C}$. The samples, taken out at established time periods, were dried by lightly pressing with filter paper and stored in a desiccator with silica gel for at least 24 h before any measurement.

2.2.2 Thermooxidative Ageing

For comparison, thermooxidative ageing has been carried out on film samples (strips of $20 \times 20 \text{ cm}^2$) at 90 $^{\circ}\text{C}$ in an air circulating oven.

2.2.3 FTIR Spectroscopy

The FTIR spectra were recorded on the initial or aged films in transmission, using a Jasco FTIR 4200 spectrometer in the following conditions: spectral range 4,000–400 cm^{-1} , resolution 4 cm^{-1} , scans number 48.

The crystallinity was evaluated from FTIR data using the formula (1) [18]:

$$C \% = \frac{D}{D + \frac{K}{A}} \times 100 \quad (1)$$

where $D = \frac{E_{1894}}{E_{1300}}$, E_x is the extinction of the mentioned bands, K is the extinction coefficient for a completely crystalline 6.2 cm^{-1} polyethylene and A is the similar coefficient for a completely amorphous polyethylene.

The infrared spectra of the thermooxidized samples were recorded, in transmission, on Shimadzu 8300 FTIR spectrometer in similar conditions of spectral acquisition. The equivalence of spectral information from both spectrometers was checked by comparative measurements on initial and aged samples.

The carbonyl index (CI) has been calculated with the Eq. (2) [31]:

$$CI = \frac{A_{C=O}}{d} \times 100 \quad (2)$$

where $A_{C=O}$ is the carbonyl absorbance, typically measured at $1,720 \text{ cm}^{-1}$ and d is the film thickness in cm. In our calculations, the $A_{C=O}$ was taken at the maximum of the peak in the region $1,700 \text{ cm}^{-1}$.

2.2.4 Chemiluminescence (CL)

Chemiluminescence measurements were performed in isothermal conditions ($T = 190^\circ\text{C}$), using a Lumipol 3 (Slovak Academy of Science, Slovakia) instrument. The sample weight was ca. 2 mg, and the atmosphere surrounding sample was stagnant air.

The oxidation induction time (OIT), the time to reach half of maximum of CL intensity ($t_{1/2}$), the time to reach the maximum of the CL intensity (t_m), the oxidation rate (v_{ox}), the maximum of CL intensity (I_{max}) and the initial CL intensity (I_0) were used as kinetic parameters for characterization the oxidation processes at 190°C . The calculation procedures for these parameters as well as their significance were discussed in an earlier paper [32].

2.2.5 Differential Scanning Calorimetry (DSC)

DSC (Differential Scanning Calorimetry) measurements were performed in isothermal mode on a Setaram 131 EVO (Setaram Instrumentation, France) apparatus, using $30 \mu\text{L}$ aluminium crucibles with pierced caps. The sample weight was ca. 2 mg.

Two types of DSC measurements were performed on each sample, namely a ramp heating (10 K/min.) from room temperature up to 190°C , under inert (nitrogen) atmosphere and

an isothermal measurement (at 190°C) under air atmosphere. The gas flow was 50 mL/min for both types of measurements. Typical DSC curves for polyethylene in both nitrogen and air atmosphere were presented in paper [33], together the parameters which can be calculated from. The small exothermic peaks observed between 120 and 170°C were assigned to hydroperoxide decomposition [34–36].

When the measuring temperature was reached, the nitrogen atmosphere was kept for 5 min, then the gas flow was switched on air (50 mL/min). The zero-moment of the measurement in oxidizing atmosphere was considered the moment of nitrogen to air switching. The DSC curve recorded in these conditions was used to determine the oxidation induction time (OIT), the time to reach the maximum of the oxidation peak (t_{max}) and the oxidation enthalpy (ΔH_{ox}). The OIT was calculated according to ASTM D 3895-07 [37] as the cross point of the recorded baseline and the slope of the oxidation exotherm, using the specific OIT function of Calisto Data Processing (CDP) software.

Other parameters were calculated using the CDP function *Integration*. Tangential first point mode has been chosen to draw the baseline of the integral.

The crystallinity was calculated as the ratio of the observed thermal effect of the melting process (ΔH_m) and the thermal effect of the melting of a completely crystalline polyethylene sample i.e. 285 J/g [38,39]. In the case of the peaks containing a shoulder or a relative maxim, the whole thermal effect assigned to the crystallinity melting was considered.

2.2.6 X-ray Diffraction (XRD)

The XRD spectra were recorded by a XPert Pro-Panalytical diffractometer, type MPD/vertical system, using $\text{Cu K}\alpha$ radiation with $\lambda = 1.54 \text{ \AA}$.

2.2.7 Scanning Electron Microscopy (SEM)

The examination of the surface of the film samples, before and after ageing, was performed by a Quanta 200 SEM instrument operating in environmental mode at 10 – 12.5 kV . This instrument enables the investigation of non-conductive samples without any prior conditioning.

3 Results and Discussion

3.1 FTIR Analysis and SEM Exploration

The spectra of the hydrothermally aged samples presented significant increase of absorption in the bands related to the degradation of the polymer, especially of those assigned to carbonyl and hydroxyl groups (see Fig. 1). The general increase in the absorbance in the region of $3,400 \text{ cm}^{-1}$

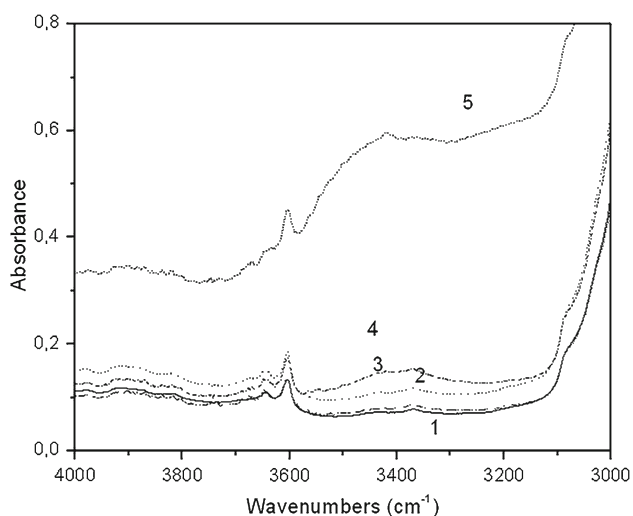


Fig. 1 FTIR transmission spectra, in the region 4,000–3,000 cm^{-1} of LDPE films exposed to hydrothermal ageing for different time periods: 1 unaged; 2 21 days; 3 42 days; 4 54 days; 5 71 days

includes the absorbance at 3,420 cm^{-1} (OH in associated hydroperoxides [40]) and 3,371 cm^{-1} (OH in alcohols [40]) indicating an intense oxidative degradation process.

The occurrence of large amounts of OH groups as a result of the hydrothermal ageing is also confirmed by the peaks at 1,010 and 1,177 cm^{-1} . The former peak is assigned to primary alcohols [41]. As this band is quite wide, the occurrence of other types of alcohols (secondary or tertiary) is possible. This peak does not exist in the initial polymer, but appeared immediately after the beginning of hydrothermal ageing; further periods, it remained more or less constant. The peak at 1,177 cm^{-1} , assigned to C–O bonds in alcohols [42], has similar evolution, both peaks suggesting the production of alcohol groups during the hydrothermal ageing of the polyethylene film.

In the spectral region 2,200–1,000 cm^{-1} , a dramatic increase of the band at 1,700 cm^{-1} is observed for LDPE (Fig. 2). The shoulders and the relative maxims on this carbonyl band (with an absolute maximum at 1,712 cm^{-1}) indicated the occurrence of similar oxidized groups as observed for high-temperature oxidized PE samples in presence of air or oxygen [41]. Thus, γ -lactones (1,796 cm^{-1} [41]), peracids (1,777 and 1,666 cm^{-1} [43,44]), esters (1,740 cm^{-1} [41]), aldehydes (1,730 cm^{-1} [41,42]), ketones (1,720 cm^{-1} [40,44–47]), carboxylic acids (1,710 cm^{-1} , [40,41,44]), α - and β -unsaturated acid (1,702 cm^{-1} [47]) and unsaturated ketones (1,690 cm^{-1} and 1,675 cm^{-1} [41]) were observed. Among these groups, those corresponding to γ -lactones, peracids or esters occurred already in the initial unaged films due to possible oxidation processes during the films manufacturing. While the γ -lactones and peracids remained practically constant, the esters increased similar to other groups such as ketones or acids. In the initial film, the

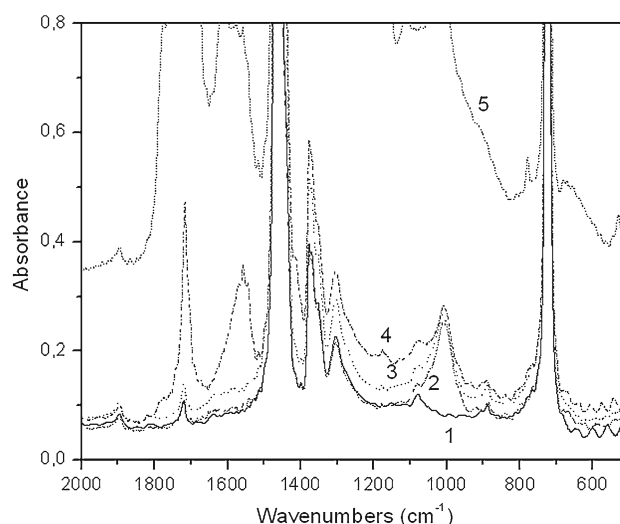


Fig. 2 FTIR transmission spectra, in the region 2,000–500 cm^{-1} of LDPE films exposed to hydrothermal ageing for different time periods: 1 unaged; 2 21 days; 3 42 days; 4 54 days; 5 71 days

ketone peak at 1,720 cm^{-1} is the most intense in this spectral region, while the acid group concentration is rather low. Finally, the concentration level of both the acid groups (1,710 and 1,700 cm^{-1}) and unsaturated ketones (1,690 and 1,675 cm^{-1}) increased considerably during the ageing treatment (Fig. 2), so that the acid peak at 1,712 cm^{-1} is the absolute maximum of the 1,700 cm^{-1} band.

A peak at 1,612 cm^{-1} can be assigned to the carbon double bonds in different oxidized unsaturated compounds. The occurrence of this peak is consistent with the strong increase of the peak at 935 cm^{-1} (vinyl terminal groups [40]) as well as to the increase of other peaks related to the occurrence of double bonds, such as 966 cm^{-1} (transvinylene groups) [40].

Other peaks at 1,412 and ca. 670 cm^{-1} indicate as well the presence of internal ketones [41].

For the samples stabilized with PR 31, no significant hydrothermally induced degradation has been observed comparatively to the unstabilized reference sample. Thus, no significant increase of both OH and carbonyl peaks and no peaks appeared at 1,177 cm^{-1} (C–O in ethers) as shown in Fig. 3. The absence of the peak at 1,177 cm^{-1} suggests the inhibition of the crosslinking reactions of PE chains produced by HALS by trapping the macroradicals of polyethylene.

The peak at 1,010 cm^{-1} has the same evolution as in the case of the reference LDPE sample, i.e. sudden increase and minor variation afterwards. This behaviour suggests that the OH groups are primarily products of degradation, other groups resulting by successive reactions of these groups.

No shifting of the baseline in infrared was observed as well for PR 31-containing sample, furthermore suggesting the interference of this HALS in the degradation mechanism.

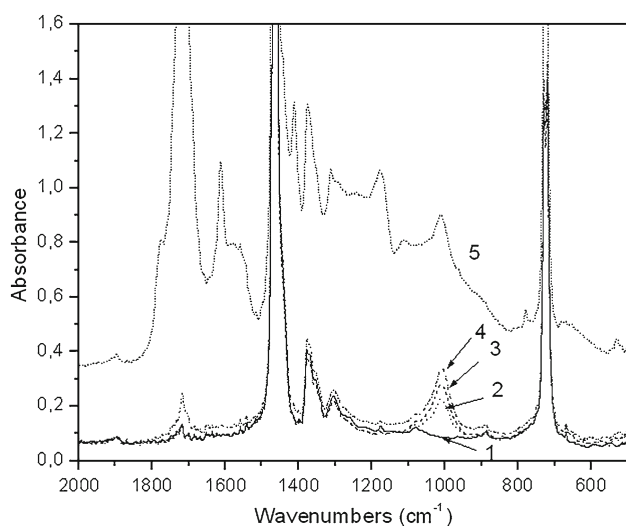


Fig. 3 FTIR transmission spectra, in the region 2,000–500 cm^{-1} of LDPE films stabilized with Sanduvor PR 31 and exposed to hydrothermal ageing for different time periods: 1 unaged; 2 42 days; 3 56 days; 4 98 days; 5 for comparison, the unstabilized sample aged in same conditions for 71 days

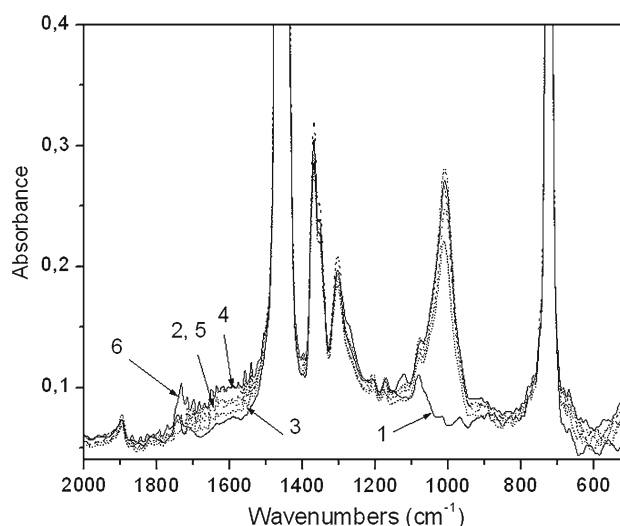


Fig. 5 FTIR transmission spectra, in the region 2,000–500 cm^{-1} of unstabilized mLLDPE films exposed to hydrothermal ageing for different time periods: 1 unaged; 2 85 days; 3 110 days; 4 135 days; 5 194 days; 6 228 days

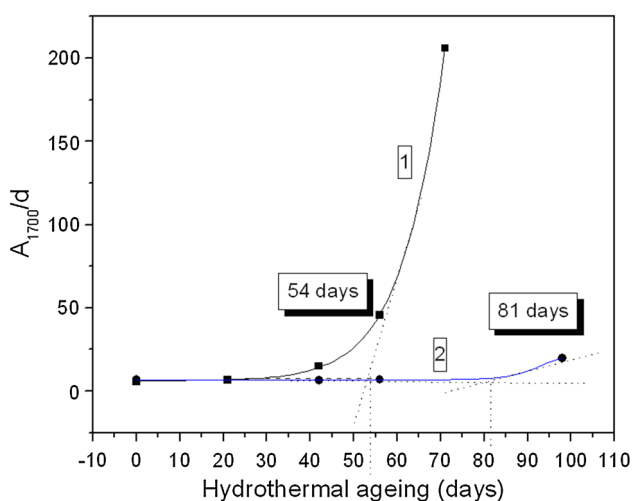


Fig. 4 Carbonyl index as a function of the hydrothermal ageing time for LDPE reference sample (1) and LDPE + 0.3% PR 31 (2)

Comparative plotting of the carbonyl index showed that there is an induction period for carbonyl formation of about 54 days for LDPE and 81 days for LDPE containing 0.3 wt% of PR 31 (Fig. 4). Similar results were obtained in the case of double bond content at 965 cm^{-1} .

Hence, the stabilization effect of the mentioned HALS can be quantitatively characterized.

No significant changes were observed in the FTIR spectra of mLLDPE (Fig. 5) and mLLDPE + PR 31, up to 228 days of exposure to hydrothermal degradation, excepting some small changes in the regions of 3,000–3,600 and 1,700 cm^{-1}

(a small peak at 1,733 cm^{-1} presented higher intensity for long-term aged samples).

The dramatic increase of LDPE sample's absorbance exposed for 71 days at hydrothermal degradation is thought to be in relation to its intense degradation. Visibly, it presented a low transparency and poor mechanical properties (the film is fairly brittle). This behaviour could be related to an increase in crystallinity as a result of chain scission processes. However, the measured crystallinity level increased, but not in such an extent. Therefore, we assumed that oxidative degradation of the polymer, especially in the surface region, is responsible for this general increase of the LDPE opacity. It should be noticed that this assumption has been confirmed by SEM measurements that clearly indicated the presence of deep crevices on the surface of sample aged for 71 days in hydrothermal conditions (Fig. 6). This effect was no visible for other samples, namely HALS-stabilized LDPE or mLLDPE (Fig. 7).

This behaviour which is significantly different to that of LDPE indicates a remarkable stability of the base polymer mLLDPE. However, the peak at 1,010 cm^{-1} presented similar evolution.

The carbonyl index values proved that the effect of hydrothermal ageing at 90 °C was significantly more intense than the effect of thermal oxidation at the same temperature as shown the data in Table 1.

The effect of the polymer structure can be also observed through the comparison of the values of induction time as shown in Table 1. Increased stability is observed for the mLLDPE-based samples due to its more regulated structure.

Fig. 6 The SEM images of the surface of LDPE films before hydrothermal ageing (a), after 71 days of hydrothermal ageing (b, c). The micrograph (d) presents, for comparison, the surface of the LDPE-PE 31 film after 98 days of hydrothermal ageing. The magnification: 1,000 for micrographs (a) and (b) and 8,000 for (c) and (d)

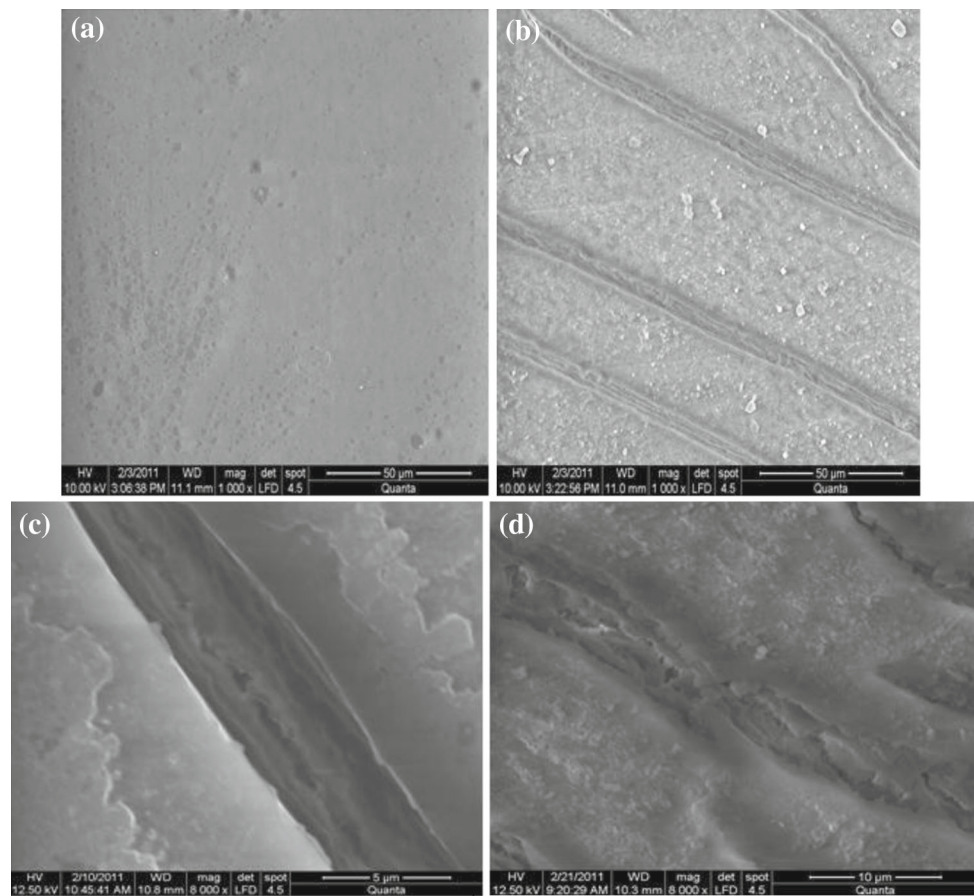


Fig. 7 The SEM images of the surface of mLLDPE films before (a) and after 217 days of hydrothermal ageing (b). The magnification: 1,000

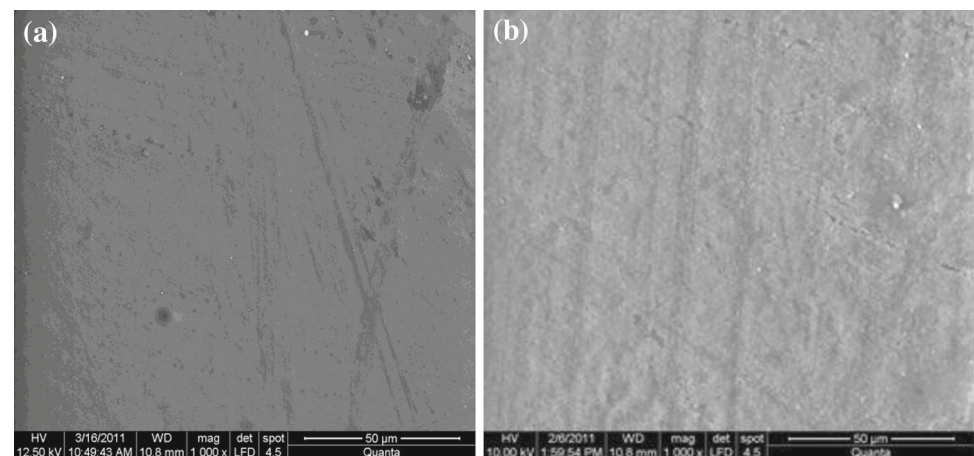


Table 1 The values of the induction time for carbonyl index increase in LDPE and mLLDPE subjected to degradation in either stabilized or unstabilized state

Degradation type	Induction time of carbonyl index increase			
	LDPE	LDPE + PR 31	mLLDPE	mLLDPE + PR 31
Thermooxidative	105	>120	>120	>120
Hydrothermal	54	81	143	192

The stabilization effectiveness of PR 31 in hydrothermal ageing appears lower in the case of mLLDPE versus LDPE, if the ratios of the induction times (IT) in the stabilized and

unstabilized states (IT_{stab}/IT_0) are compared, i.e. for LDPE the ratio's value is 1.5 while for mLLDPE it is around 1.3. This behaviour can be assigned to the regulated structure

of mLLDPE which results in higher stability of the polymer chain and, consequently, in less opportunities for HALS grafting.

3.2 Crystallinity

The crystallinity levels were evaluated by three different techniques (FTIR, XRD and DSC) in order to better understand the behaviour of the samples. Even though the results concerning a certain sample were inherently different, depending on the method used, the general trends (as resulted from the averaging of crystallinity data for each sample) were remarkably clear. In the case of LDPE, the crystallinity tends to slightly increase as increases the ageing time (Fig. 8). At

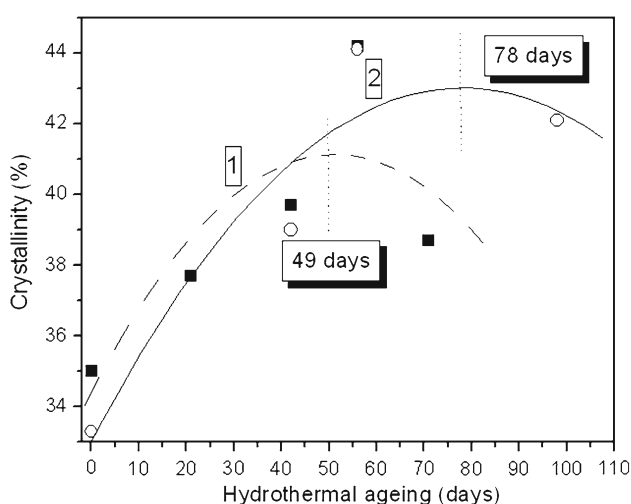
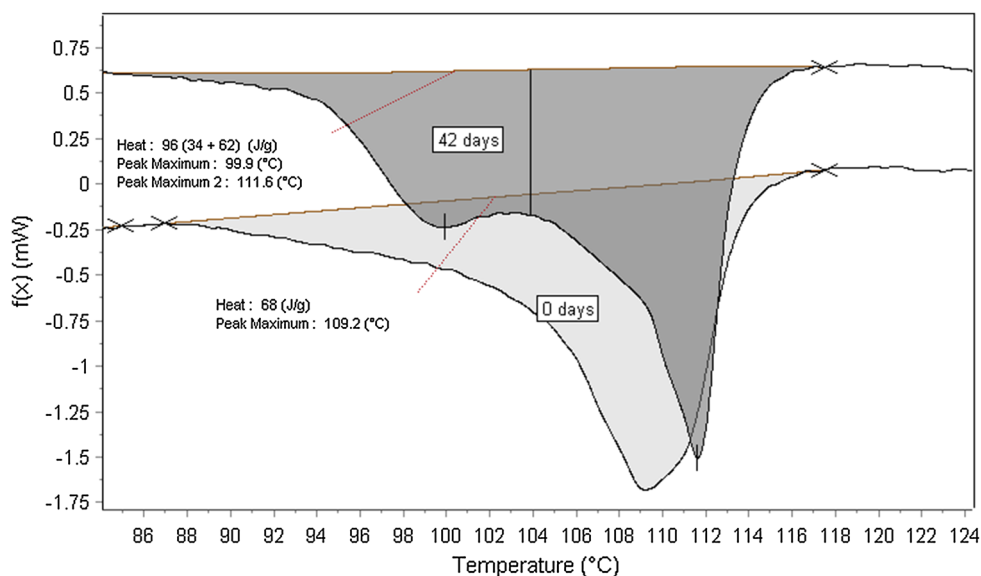


Fig. 8 Crystallinity versus the duration of hydrothermal ageing for LDPE-based samples: 1 (filled square)—free of PR 31 LDPE (reference); 2 (open circle)—LDPE + 0.3% Sanduvor PR 31

Fig. 9 The melting process of LDPE reference sample, as observed in DSC for the unaged sample and for the thermally aged sample for 42 days



high degradation levels, the crystallinity tends to decrease, possibly as a result of chemical changes observed in infrared spectra. Similar behaviour was observed for the PR 31-containing sample, but the maximum of the crystallinity appears later than for reference LDPE. The increase in crystallinity can be assigned to both relaxation of the polymer chains in hydrothermal conditions and thermally induced scissions in the amorphous regions leading to deterioration of the mechanical properties.

In DSC thermograms were observed not only changes in the melting heat (which increases with the ageing time), but also different shape of the melting peak: a second peak at lower temperature was observed (see Fig. 9), this effect being more intense in the case of free of PR 31 sample. This peak suggests the formation of a crystalline phase which would be less ordered than the initial one, due to the vicinity of oxidized groups.

The mLLDPE presented a similar behaviour from point of view of its crystallinity as the LDPE samples: the crystallinity increased steadily with the ageing time up to around 100 days of ageing. Then, it tends to decrease. The presence of PR 31 results in lower crystallinity levels, as well as in shifting of the crystallinity maxim to around 130 days (Fig. 10).

Taking into account the low intensity of the chemical changes observed in FTIR spectra for these samples, it can be assumed that the observed changes in crystallinity are due to physical ageing of polymer rather to chemical transformations. Hence, till the moment of reaching the maximum of crystallinity, thermally induced re-arrangement of the polymer chains is possibly the main process. Afterward, swelling effects associated to chemical transformations (scission of alkyl side groups, and hydro-oxidative degradation reactions) can predominate leading to less ordered structures.

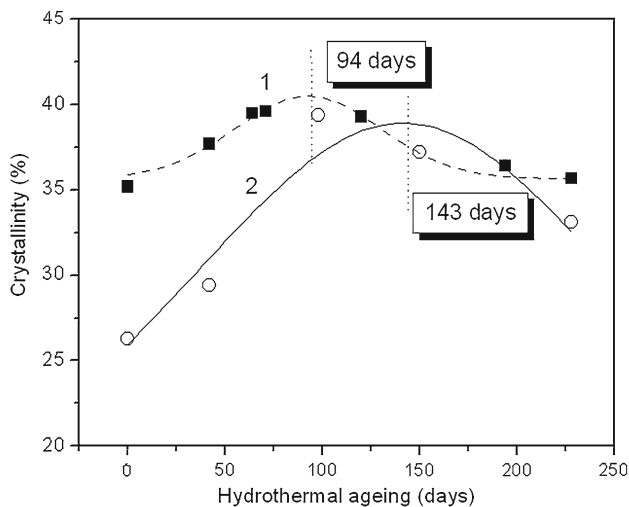


Fig. 10 Crystallinity versus the duration of hydrothermal ageing for mLLDPE-based samples: 1 (filled square)—free of PR 31 mLLDPE (reference); 2 (open circle)—mLLDPE + 0.3 % Sanduvor PR 31

3.3 Chemiluminescence

Chemiluminescence was proven as a very sensitive technique in detection of early oxidation stages in different stress conditions [32] as well as in understanding of degradation and stabilization mechanisms. Hence, this technique was used in this work in order to characterize both the differences between the behaviours of the studied materials and the effect of the HALS compound.

The CL data presented in Tables 2, 3, 4 and 5 indicate a clear stabilization effect of PR 31 in the case of LDPE samples, while in the case of mLLDPE, this effect is less clear, being masked probably by the presence of a processing antioxidant which provided high OIT values as well as by a possible antagonism between these two stabilizers.

The oxidation induction time values (OIT) for LDPE samples decreased as function of the ageing time for all types of studied materials after a certain period of exposition to hydrothermal conditions.

For LDPE reference samples, the initial OIT values (Table 2) were low, but these values remained practically constant with the ageing time for relative long time periods: the zero value of OIT is reached after 42 days of ageing.

The OIT values of the LDPE + PR 31 samples decreased less rapidly as compared to the reference sample (Table 3).

In the case of mLLDPE, considerably longer OIT values are observed for reference and mLLDPE + PR 31 samples as compared to the LDPE counterparts (Tables 4, 5).

The effect of stabilizer, PR 31, on hydrothermal behaviour of LDPE samples can be also described by t_{\max} values. As it can be seen in Fig. 11, t_{\max} decreased slower in presence of the stabilizer as compared to the free of PR 31 sample. Higher value of t_{\max} for long-term aged samples was also observed as compared to the reference one.

Similar plots for mLLDPE (Fig. 12) showed that the ageing times corresponding to sudden decrease of t_{\max} values are similar to those for LDPE samples, but the residual t_{\max} values for long-term ageing are considerably higher for mLLDPE materials (Fig. 13).

The initial CL signal (I_0), due to hydroperoxides and free radicals induced during the sample history, increased with the duration of the hydrothermal ageing of LDPE-based samples (Tables 2, 3). There is an induction period of 56 days for this increase (during this period, I_0 remains practically constant) in the case of LDPE + PR 31, while in the case of LDPE (free of HALS), the signal increased proportionally to the ageing time. The value of I_0 is considerably higher for LDPE samples as compared to the corresponding LDPE + PR 31 ones, indicating clearly the role of HALS in material stabilization: lower content in chemiluminescence emitting species, i.e. less free radicals and hydroperoxides are observed for LDPE + PR 31 samples.

I_0 values increased also with the ageing time for mLLDPE reference samples, reaching a maximum after 76 days (Table 4). Generally, these values are higher than that in the case of LDPE reference samples, suggesting the presence of an additive or impurity, which enhances the CL efficiency.

Table 2 The kinetic parameters of isothermal oxidation of LDPE reference samples from CL measurements at 190 °C, air stagnant

Ageing time (days)	m (mg)	OIT (min)	t_{\max} (min)	$I_0 \cdot 10^{-4}$ (Hz)	$I_{\max} \cdot 10^{-7}$ (Hz)	v_{ox} (%/min)
0	2.7	6.7	124	0.46	3.2	1.1
42	3.8	6.9	112	1.48	5.8	1.35
54	3.4	5.0	26	14.10	10.9	4.29
71	4.4	0.0	5	58.90	14.7	27.09

Table 3 The kinetic parameters of isothermal oxidation of LDPE + PR 31 samples from CL measurements at 190 °C, air stagnant

Ageing time (days)	m (mg)	OIT (min)	t_{\max} (min)	$I_0 \cdot 10^{-4}$ (Hz)	$I_{\max} \cdot 10^{-7}$ (Hz)	v_{ox} (%/min)
0	2.4	4.8	112	0.51	1.87	1.47
42	3.1	11.2	116	0.67	1.15	1.04
56	2.2	0.0	112	0.40	0.70	1.22
98	2.2	0.0	35	10.37	0.05	8.71

Table 4 The kinetic parameters of isothermal oxidation of mLLDPE reference samples from CL measurements at 190 °C, air stagnant

Ageing time (days)	m (mg)	OIT (min)	t_{max} (min)	$I_0 \cdot 10^{-4}$ (Hz)	$I_{max} \cdot 10^{-7}$ (Hz)	v_{ox} (%/min)
0	2.3	138	218	100	7.52	2.66
42	2.3	85	207	179	8.45	1.89
76	2.0	32	110	201	11.90	3.92
98	2.4	22	83	132	13.50	2.19

Table 5 The kinetic parameters of isothermal oxidation of mLLDPE + PR 31 samples from CL measurements at 190 °C, air stagnant

Ageing time (days)	m (mg)	OIT (min)	t_{max} (min)	$I_0 \cdot 10^{-4}$ (Hz)	$I_{max} \cdot 10^{-7}$ (Hz)	v_{ox} (%/min)
D0	2.0	142	228	51.5	8.11	1.24
D42	2.7	81	243	15	695	0.91
D76	2.2	39	120	9.4	1.14	1.23
D98	2.5	14	79	7.9	12.90	1.89
D120	3.1	27	79	44	4.95	2.36
D135	2.8	9	61	90	10.50	3.3

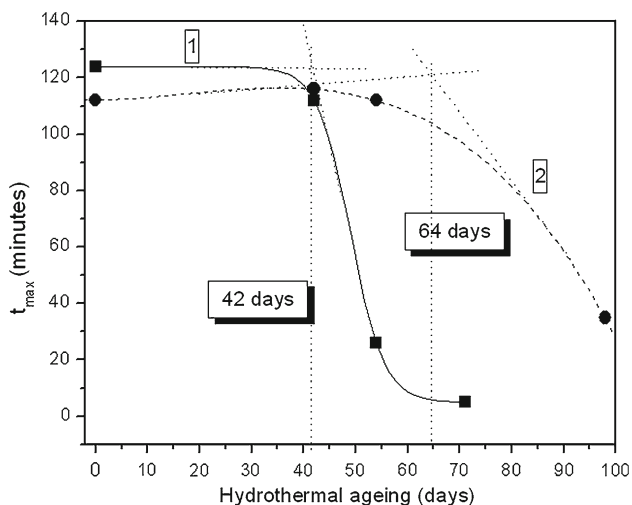


Fig. 11 Dependence of t_{max} parameter from CL on the hydrothermal ageing time for LDPE reference sample (1) and LDPE + 0.3% PR 31 (2)

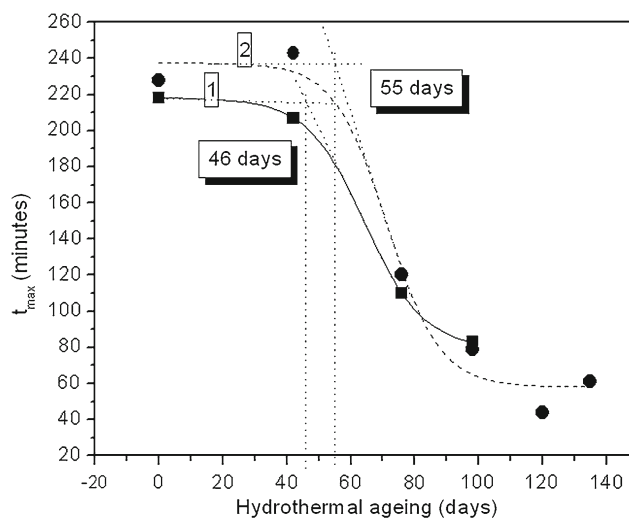


Fig. 12 Dependence of t_{max} parameter from CL on the hydrothermal ageing time for mLLDPE reference sample (1) and mLLDPE + 0.3% PR 31 (2)

Similar to the case of LDPE, lower I_0 values were observed for mLLDPE samples containing PR 31, indicating the interference of this compound in the degradation mechanism (Tables 4, 5).

The values of the initial CL signals for all aged samples are consistent with the observed increase in optical absorption in FTIR at $3,420\text{ cm}^{-1}$ and confirm that oxidation plays an important role in the present hydrothermal degradation process.

In the case of other CL parameter, I_{max} which is related to the concentration of oxidation-active sites, there is also a clear difference between LDPE reference and LDPE + PR 31 samples: while the I_{max} values increased for the reference samples as the ageing time increased (indicating an increase in oxidation susceptibility), a decrease in I_{max} as the ageing time increased was observed for the stabilized LDPE samples. The lower oxidation susceptibility of these samples can

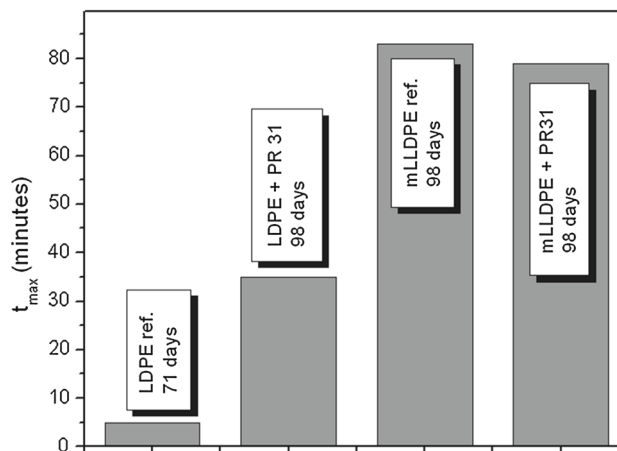


Fig. 13 Comparison of the t_{max} (from CL) values for long-term aged (th ageing time is indicated for each sample on the figure) samples in hydrothermal conditions

be assigned to a possible HALS grafting process that compete the decrease in sample stability induced by HALS leaching and oxidation.

I_{\max} increased also for mLLDPE samples with the ageing time, while a less clear trend was observed for mLLDPE + PR 31 samples: in this case, the signal was rather constant, possibly due to less HALS tendency to induce crosslinking as compared to LDPE sample.

In the case of LDPE-based samples, the oxidation rate values increased as the ageing time increases, but the process was more rapid for LDPE reference samples. The values of oxidation rate corresponding to a same ageing time are considerably higher for these samples as compared to LDPE + PR 31 ones, indicating a higher stability of HAS-containing samples. As for example, the ratio of the oxidation rates of LDPE reference and LDPE + PR 31 samples is around 6 for the samples aged 71 days.

For mLLDPE-based samples, the values of the oxidation rate are practically independent on the ageing state, suggesting a lower oxidation stability of this polymer in the auto-catalysed phase of oxidation (when the stabilizers are chemically depleted).

3.4 Differential Scanning Calorimetry

Besides the melting of crystallinity that was discussed above, the DSC curves in inert atmosphere presented some weak exotherm peaks in the range 120–170 °C, which can be related to the hydroperoxide content of the sample as it was already mentioned. Generally, for all samples, on this range, the total heat (ΔH_{150}) increased at the beginning with the ageing time and then decreased (Fig. 14), possibly as a result of hydroperoxide decomposition, either by vicinal reactions (at high concentrations) or by their decomposition by stabilizers. However, higher values of this heat were observed in LDPE reference samples and no level-off was observed in this case. For LDPE + PR 31, the ΔH_{150} present higher values than for mLLDPE samples, suggesting a higher stability of the latter ones, in good agreement with the above results. It is interesting to remark that the data of ΔH_{150} versus ageing time can be linearly fitted for the reference samples, while a second-order polynomial fitting is the case of PR 31-containing samples (Fig. 14), suggesting a different mechanism of hydroperoxide formation and decomposition in presence of HAS.

For the isothermal measurements, the temperature was the same as in CL measurements. However, due to possible influence of dynamic atmosphere influence, the oxidation was considerably more intense than in CL measurements. As a result, the OIT values were small and only the t_{\max} values were measured.

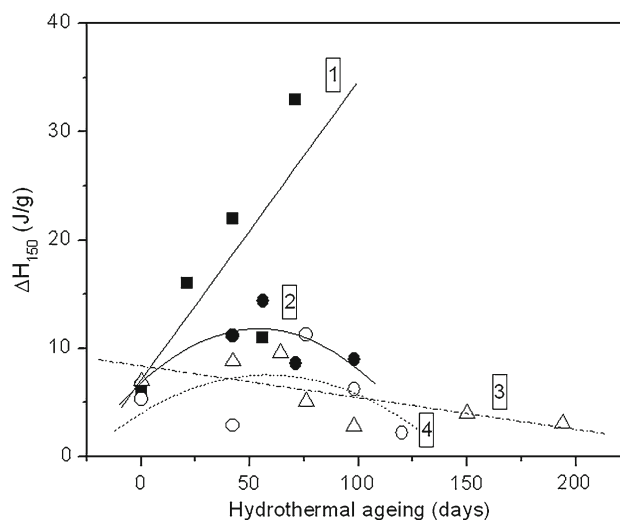


Fig. 14 The heat in the range 130–170 °C (ΔH_{150}) versus hydrothermal ageing time for different polyethylene films: 1 (filled square) LDPE reference; 2 (filled circle) LDPE + PR 31; 3 (open triangle) mLLDPE reference; 4 (open circle) mLLDPE + PR 31

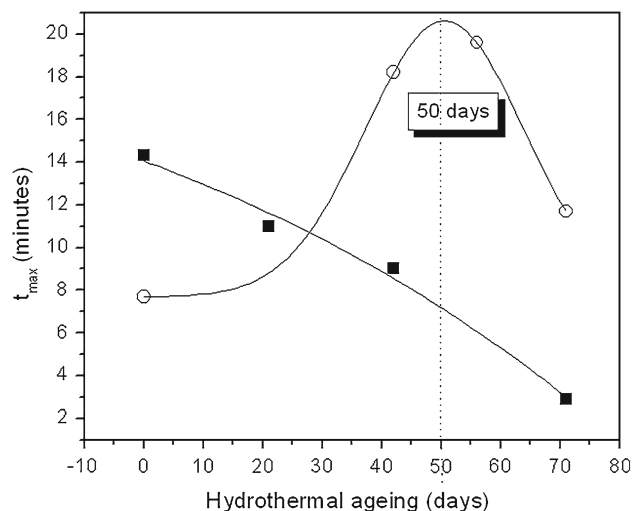


Fig. 15 Dependence of t_{\max} parameter from DSC on the hydrothermal ageing time for LDPE reference sample (1) and LDPE + 0.3 % PR 31 (2)

For LDPE reference sample, the decrease of t_{\max} values was practically linear with ageing time (Fig. 15), while in the case of LDPE + PR 31, the initial increase of t_{\max} suggests an increase in stability due to possible grafting of the stabilizer induced by hydrothermal ageing.

For mLLDPE samples, the effect of the stabilizer was less clear, as compared to the reference sample, but an initial increase of the stability of aged samples was also observed (Fig. 16). Generally, the isothermal DSC measurements confirmed the higher stability of mLLDPE films in hydrothermal ageing as compared to LDPE films, but no clear effect of the PR 31 was evidenced in mLLDPE.

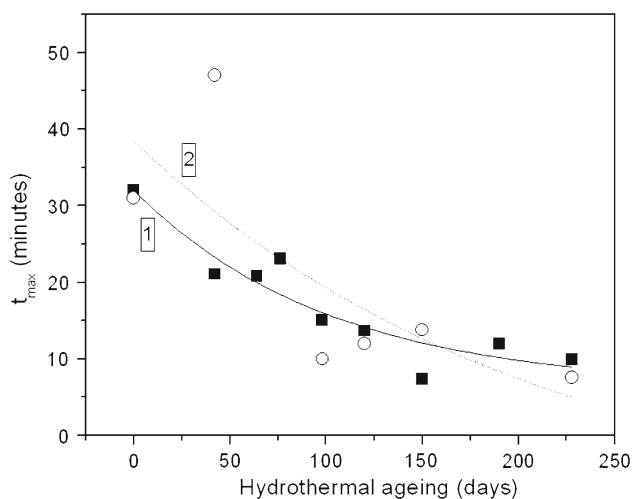


Fig. 16 Dependence of t_{\max} parameter from DSC on the hydrothermal ageing time for mLLDPE reference sample (1) and mLLDPE + 0.3 % PR 31 (2)

4 Conclusions

Hydrothermal ageing of polyethylene films at 90 °C in distilled water involves oxidative degradation processes leading to carboxylic acid and ketone groups on the aged polymer chain. Significant amounts of unsaturated compounds were also observed for LDPE reference films.

mLLDPE reference films presented considerably higher stability as compared to LDPE, due to both structural peculiarities and different stabilization.

The HALS compound Sanduvor PR 31 induced higher stability in LDPE, possibly by grafting mechanism, but it did not present a significant effect in the case of mLLDPE. Besides a possible antagonist interaction with the process stabilizer or a graft-hindering effect of the alkyl side groups, the intrinsic higher stability of the mLLDPE which offers less active sites for grafting could be supposed to explain the lower effectiveness of PR 31 in this case.

The connection of oxidative degradation under thermal ageing to the durability of investigated materials emphasizes the necessity of detailed information of handling for their long-term usage. The influence of hydrothermal factors on material stability must be deeply known for their proper selection envisaging both high stability and adequate environmental behaviour.

Acknowledgments The authors are grateful to the Romanian Ministry of Education, Research and Youth for the financial support Granted through the Project GR-10-EU 2011.

References

1. Verdu, J.: Vieillissement des Plastiques. Paris, AFNOR (1984)

- Foster, G.N.; Wasserman, S.H.; Yacka, D.J.: Oxidation behavior and stabilization of metallocene and other polyolefins. *Angew. Makromol. Chem.* **252**, 11–32 (1997)
- Zweifel, H.: Stabilization of Polymeric Materials. Springer, Berlin (1998)
- Pospíšil, J.: Mechanistic action of phenolic antioxidants in polymers—a review. *Polym. Degrad. Stab.* **20**, 181–202 (1988)
- Scott, G.: Atmospheric Oxidation and Antioxidants. Elsevier, London (1993)
- Scott, G.: Mechanism of polymer stabilization. *Pure Appl. Chem.* **30**, 267–289 (1972)
- Al-Malaika, S.; Omikorede, E.O.; Scott, G.: Mechanisms of antioxidant action: Mechanochemical transformation products of 2,2,6,6-tetramethyl-4-hydroxy-piperidinoxyl in polypropylene. *J. Appl. Polym. Sci.* **33**, 703–713 (1987)
- Gijsman, P.: The mechanism of action of hindered amine stabilizers (HAS) as long-term heat stabilizers. *Polym. Degrad. Stab.* **43**, 171–176 (1994)
- Kerboua, N.; Moussaceb, K.; Kaci, M.; Benachour, D.; Sadoun, T.; Rouba, N.: Modeling of the kinetic degradation of unstabilized and HALS-stabilized LDPE films in natural aging. *Arab. J. Sci. Eng.* **36**, 541–552 (2012)
- He, W.; Li, G.; Kong, L.; Wang, H.; Huang, J.; Xu, J.: Application of hydrothermal reaction in resource recovery of organic wastes. *Resour. Conserv. Recycl.* **52**, 691–699 (2008)
- Viebke, J.; Gedde, U.W.: Assessment of lifetime of hot-water polyethylene pipes based on oxidation induction time data. *Polym. Eng. Sci.* **38**, 1244–1250 (1998)
- Viebke, J.; Hedenqvist, M.; Gedde, U.W.: Antioxidant efficiency loss by precipitation and diffusion to surrounding media in polyethylene hot-water pipes. *Polym. Eng. Sci.* **36**, 2896–2904 (1996)
- Gedde, U.W.; Ifwarson, M.: Molecular structure and morphology of crosslinked polyethylene in an aged hot-water pipe. *Polym. Eng. Sci.* **30**, 202–210 (1990)
- Dörner, G.; Lang, R.W.: Influence of various stabilizer systems on the ageing behavior of PE–MD: I. Hot-water ageing of compression molded plaques. *Polym. Degrad. Stab.* **62**, 421–430 (1998)
- Mittelman, G.; Davidson, J.H.; Mantell, S.C.; Su, Y.: Prediction of polymer tube life for solar hot water systems: a model of antioxidant loss. *Solar Energy* **82**, 452–461 (2008)
- Mueller, W.; Jakob, I.: Oxidative resistance of high-density polyethylene geomembranes. *Polym. Degrad. Stab.* **79**, 161–172 (2003)
- Sangam, H.P.; Kerry Rowe, R.: Effects of exposure conditions on the depletion of antioxidants from high-density polyethylene (HDPE) geomembranes. *Can. Geotech. J.* **39**, 1221–1230 (2002)
- Rowe, K.R.; Rimal, S.: Aging of HDPE geomembrane in three composite landfill liner configurations. *J. Geotech. Geoenviron. Eng.* **134**, 906–916 (2008)
- Rimal, S.; Rowe, R.K.: Diffusion modelling of OIT depletion from HDPE geomembrane in landfill applications. *Geosynth. Int.* **16**, 183–196 (2009)
- Rowe, R.K.; Hoor, A.: Predicted temperatures and service lives of secondary geomembrane landfill liners. *Geosynth. Int.* **16**, 71–82 (2009)
- Rowe, K.R.; Islam, M.; Hsuan, Y.: Effects of thickness on the aging of HDPE geomembranes. *J. Geotech. Geoenviron. Eng.* **136**, 299–309 (2010)
- Avissar, R.; Mahrer, Y.; Margulies, L.; Katan, J.: Field aging of transparent polyethylene mulches: I. Photometric properties. *Soil Sci. Soc. Am. J.* **50**, 202–205 (1986)
- Guerhazi, N.; Elleuch, K.; Ayedi, H.F.; Kapsa, P.: Aging effect on thermal, mechanical and tribological behaviour of polymeric coatings used for pipeline application. *J. Mater. Process. Technol.* **203**, 404–410 (2008)



24. Boubakri, S.; Elleuch, K.; Guermazi, N.; Ayedi, H.F.: Investigations on hygrothermal aging of thermoplastic polyurethane material. *Mater. Design*. **30**, 3958–3965 (2009)
25. Albertsson, A.C.; Barenstedt, C.; Karlsson, S.: Abiotic degradation products from enhanced environmentally degradable polyethylene. *Acta Polym.* **45**, 97–103 (1994)
26. Kaci, M.; Hebal, G.; Benhamida, A.; Boukerrou, A.; Djidjelli, H.; Sadoun, T.: Kinetic study of hindered amine light stabilizer photografting in low density polyethylene films under natural weathering conditions. *J. Appl. Polym. Sci.* **84**, 1524–1532 (2002)
27. Kaci, M.; Hebal, G.; Touati, M.; Rabouhi, A.; Zaidi, L.; Djidjelli, H.: Kinetic study of hindered amine light stabilizer photografting in poly(propylene) films under natural weathering and accelerated UV conditions: effect of additive concentration. *Macromol. Mater. Eng.* **289**, 681–687 (2004)
28. Kaci, M.; Touati, N.; Setnescu, R.; Setnescu, T.; Jipa, S.: Characterization by chemiluminescence of unstabilized and HALS-stabilized LDPE films exposed to natural weathering conditions. *Int. J. Polym. Anal. Charact.* **9**, 285–287 (2004)
29. Kaci, M.; Touati, N.; Setnescu, R.; Zaharescu, T.; Setnescu, T.; Jipa, S.: Grafting of hindered amine stabilizer in poly(propylene) films under γ -irradiation. *Macromol. Mater. Eng.* **290**, 802–808 (2005)
30. Setnescu, R.; Kaci, M.; Jipa, S.; Setnescu, T.; Zaharescu, T.; Hebal, G.; Benhamida, A.; Djedjelli, H.: Chemiluminescence study on irradiated low-density polyethylene containing various photostabilisers. *Polym. Degrad. Stab.* **84**, 475–481 (2004)
31. Allen, N.S.; Edge, M.: *Applied Science*. Elsevier, London (1992)
32. Setnescu, R.; Jipa, S.; Osawa, Z.: Chemiluminescence study on the oxidation of several polyolefins—I. Thermal-induced degradation of additive-free polyolefins. *Polym. Degrad. Stab.* **60**, 377–383 (1998)
33. Ilie, S.D.; Setnescu, R.; Lungulescu, E.M.; Marinescu, V.; Ilie, D.; Setnescu, T.; Mareş, G.: Investigations of a mechanically failed cable insulation used in indoor conditions. *Polym. Test.* **30**, 173–182 (2011)
34. Astruc, A.; Bartolomeo, P.; Fayolle, B.; Audouin, L.; Verdu, J.: Accelerated oxidative ageing of polypropylene fibers in aqueous medium under high oxygen pressure as studied by thermal analysis. *Polym. Test.* **23**, 919–923 (2004)
35. Calvert, J.G.; Pitts, J.N.: *Photochemistry*. Wiley, New York (1966)
36. Richaud, E.; Farcas, F.; Fayolle, B.; Audouin, L.; Verdu, J.: Hydroperoxide titration by DSC in thermally oxidized polypropylene. *Polym. Test.* **25**, 829–838 (2006)
37. ASTM D 3895-07: Standard Test Method for Oxidative-Induction Time of Polyolefins by Differential Scanning Calorimetry
38. Wunderlich, B.: Heat of fusion of polyethylene. *J. Polym. Sci. A* **2**(5), 987–988 (1967)
39. Seeba, M.; Servens, C.; Pouyet, J.: Natural and artificial weathering of low density polyethylene (LDPE): calorimetric analysis. *J. Appl. Polym. Sci.* **45**, 1049–1056 (1992)
40. Bădilescu, S.; Toader, M.; Giurginca, M.; Tălpuş, V.: *Infrared Spectroscopy of Polymers and Additives* (in Roum.). Ed Tehnica, Bucharest (1982)
41. Gugumus, F.: Physico-chemical aspects of polyethylene processing in an open mixer. 2. Functional group formation on PELD processing. *Polym. Degrad. Stab.* **67**, 35–47 (2000)
42. Hariguchi, H.: *Bibliography on IR Spectra* (in Jpn.). Tokyo, Sankyo Shuppan (1989)
43. Gugumus, F.: Re-examination of the role of hydroperoxides in polyethylene and polypropylene: chemical and physical aspects of hydroperoxides in polyethylene. *Polym. Degrad. Stab.* **49**, 29–50 (1995)
44. Luongo, J.P.: Infrared study of oxygenated groups formed in polyethylene during oxidation. *J. Polym. Sci.* **42**, 139–150 (1999)
45. Amin, M.U.; Scott, G.; Tillekeratne, L.M.K.: Mechanism of the photo-initiation process in polyethylene. *Eur. Polym. J.* **11**, 85–89 (1975)
46. Adams, J.H.; Goodrich, J.E.: Analysis of nonvolatile oxidation products of polypropylene. II. Process. *Degrad. J. Polym. Sci. A* **8**, 1269–1277 (1970)
47. Carlsson, D.J.; Wiles, D.M.: The photodegradation of polypropylene films. II. Photolysis of ketonic oxidation products. *Macromolecules* **2**, 587–597 (1969)

